Environmental Science & Technology

pubs.acs.org/est

Article

Impact of a Hydrocarbon Surfactant on the Retention and Transport of Perfluorooctanoic Acid in Saturated and Unsaturated Porous Media

Yifan Ji, Ni Yan,* Mark L. Brusseau,* Bo Guo, Xilai Zheng, Mengfan Dai, Hejie Liu, and Xin Li

Cite This: https://doi.org/10.1021/acs.est.1c01919

Read Online

ACCESS | Metrics & More | Article Recommendations | Supporting Information

ABSTRACT: The transport and retention behavior of perfluorooctanoic acid (PFOA) in the presence of a hydrocarbon surfactant under saturated and unsaturated conditions was investigated. Miscible-displacement transport experiments were conducted at different PFOA and sodium dodecyl sulfate (SDS) input ratios to determine the impact of SDS on PFOA adsorption at solid−water and air−water interfaces. A numerical flow and transport model was employed to simulate the experiments. The PFOA breakthrough curves for unsaturated conditions exhibited greater retardation compared to those for saturated conditions in all cases, owing to air−water interfacial adsorption. The retardation factor for PFOA with a low concentration of SDS (PFOA−SDS ratio of 10:1) was similar to that for PFOA without SDS under unsaturated conditions. Conversely, retardation was greater in the presence of higher levels of SDS (1:1 and 1:10) with retardation factors increasing from 2.4 to 2.9 and 3.6 under unsaturated conditions due to enhanced adsorption at the solid−water and air−water interfaces. The low concentration of SDS had no measurable impact on PFOA air−water interfacial adsorption coefficients (K_{ia}) determined from the transport experiments. The presence of SDS at the higher PFOA−SDS concentration ratios increased the surface activity of PFOA, with transport-determined K_{ia} values increased by 27 and 139%, respectively. The model provided very good independently predicted simulations of the measured breakthrough curves and showed that PFOA and SDS experienced various degrees of differential transport during the experiments. These results have implications for the characterization and modeling of poly-fluoroalkyl substances (PFAS) migration potential at sites wherein PFAS and hydrocarbon surfactants co-occur.

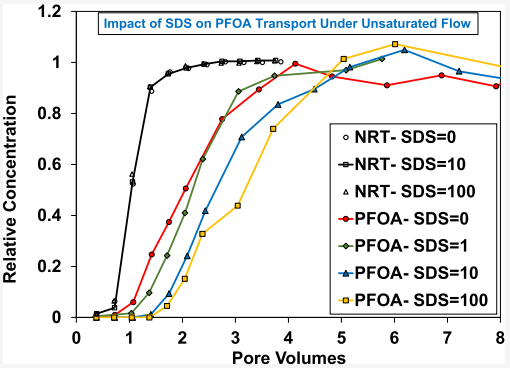

KEYWORDS: *PFAS, AFFF, hydrocarbon surfactant, air−water interfacial adsorption, surface tension*

INTRODUCTION

Per- and poly-fluoroalkyl substances (PFAS) have become an emerging concern due to their high toxicity, long-term persistence, and worldwide distribution in various environmental media including atmosphere, water, soil, sediment, wastewater, biosolids, and even remote areas such as polar glaciers.[1−5] Sites where aqueous film-forming foam (AFFF) has been used, such as firefighter training areas and crash sites, have been identified as major source zones where PFAS concentrations in soil and groundwater are comparatively high.[5−10] AFFF is a mixture of both fluorocarbon surfactants (i.e., PFAS) and hydrocarbon surfactants that has been used to extinguish fires involving hydrocarbon fuels since the 1960s.[3,11−13] Many PFAS, such as perfluorooctanoic acid (PFOA), perfluoropentanoic acid, and perfluorooctane sulfonate (PFOS), have been detected in soil and groundwater where AFFF was used.[5,6,8,14−16] Nine classes of hydrocarbon surfactants have been identified in AFFFs, such as octylphenol polyethoxylates, linear alcohol ethoxylates, alkyl sulfates, and alkyl ether sulfates.[17] It is therefore quite possible that hydrocarbon surfactants and PFAS may co-occur at some AFFF-contaminated sites. In addition, some hydrocarbon surfactants such as sodium dodecyl sulfate (SDS) are used for a wide variety of industrial, commercial, and consumer products and applications and commonly exist in wastewater and landfill leachate. Hence, it is anticipated that PFAS and surfactants such as SDS may co-occur at secondary-source contamination sites such as landfills and locations of treated-wastewater applications.

Prior field sampling and mathematical modeling have demonstrated that soil and the vadose zone at many sites are primary reservoirs of PFAS that can serve as long-term sources

Received: March 24, 2021
Revised: June 14, 2021
Accepted: July 12, 2021

to groundwater.[5,6,10,18−20] The migration of PFAS in the soil profile and vadose zone can be influenced by multiple retention processes.[21] The influence of sorption by soil on PFAS transport has been investigated in a number of studies.[22−31] In addition, laboratory and modeling studies have illustrated that retention and transport of PFAS in unsaturated porous media can be significantly affected by adsorption at air−water interfaces.[20,21,26,30,32−36] Furthermore, it has long been established that the transport of hydrocarbon surfactants in unsaturated porous media is influenced by both solid-phase sorption and air−water interfacial adsorption.[37−40] Therefore, the co-existence of hydrocarbon surfactants may have the potential to influence the retention and transport behavior of PFAS in the subsurface.

Prior studies employing batch-sorption methods have investigated the impact of hydrocarbon surfactants on the sorption of PFAS by soils. For example, the presence of a cationic surfactant, cetyltrimethylammonium bromide, enhanced the sorption of PFOS by fresh-water sediments.[41] Conversely, the influence of an anionic surfactant, sodium dodecylbenzene sulfonate, was dependent on its concentration.[41] The impact of two surfactants, SDS and *N*,*N*-dimethyldodecylamine *N*-oxide, on the sorption of 13 PFAS by three soils was investigated by Guelfo and Higgins.[42] The impacts of the hydrocarbon surfactants on PFAS sorption varied with surfactant, soil, and PFAS chain length. For example, the calculated K_d values for PFOA were larger in the presence of SDS for all three soils.

In summary, the results of the prior research indicate that the presence of hydrocarbon surfactants can influence the sorption of PFAS by soil. The presence of hydrocarbon surfactants can also influence the adsorption of PFAS at the air−water interface, as reviewed by Brusseau and Van Glubt.[43] Hence, we hypothesize that the co-occurrence of hydrocarbon surfactants may affect the transport of PFAS under unsaturated conditions via impacts to both solid-phase sorption and air−water interfacial adsorption, dependent upon the specific conditions of the system. Therefore, it is critical to investigate the interfacial behavior of PFAS in the presence of hydrocarbon surfactants under unsaturated conditions. To the best of our knowledge, the influence of hydrocarbon surfactants on the retardation and transport of PFAS has not been investigated directly via miscible-displacement studies for either saturated- or unsaturated-flow conditions.

The objective of this research is to conduct an initial investigation of the effect of hydrocarbon surfactants on the transport of PFAS in saturated and unsaturated porous media. PFOA and SDS are selected as the representative fluorocarbon and hydrocarbon surfactants, respectively. Surface tensions are measured to characterize surface activity. Miscible-displacement column experiments are conducted under saturated conditions at different PFOA and SDS input ratios to characterize solid−water interfacial adsorption, while unsaturated-flow experiments are conducted to investigate air−water interfacial adsorption. A numerical flow and transport model is employed to produce independently predicted simulations of the measured PFAS transport. The model accounts for surfactant-induced flow and multi-component solute transport influenced by nonlinear, rate-limited sorption and air−water interfacial adsorption.

MATERIALS AND METHODS

Materials. PFOA was selected as the representative PFAS because it is one of the most widely observed in both soil and groundwater and because we have conducted several studies investigating its sorption, air−water interfacial adsorption, and transport. The PFOA input concentration (C_0) was 10 μg/L for all experiments. The rationale for selecting this concentration is discussed in the Supporting Information.

SDS was selected as the representative hydrocarbon surfactant for several reasons. First, it is one of the most common surfactants in use and has been widely studied. Second, it is a reported component of AFFF, as noted in the Supporting Information. Third, its surface activity is generally similar to that of PFOA. Lastly, the sorption of SDS by the sand has been characterized in our prior study.[38]

Unlabeled PFOA (95% purity, CAS # 335-67-1) and SDS (99% purity, CAS # 151-21-3) were purchased from Sigma-Aldrich Co. $^{13}C_4$-PFOA was obtained from Wellington Laboratories Inc. Pentafluorobenzoic acid (98% purity, CAS # 602-94-8), which is neither a PFAS nor a surfactant, was obtained from Macklin Inc. (China). It was used as the nonreactive tracer (NRT) for all experiments.

The 40/50 mesh natural quartz sand with a mean diameter of 0.35 mm was washed with deionized water and then dried at 60 °C. This medium has been used in our prior studies, and thus, an extensive database exists for measured solid-phase sorption of PFOA, air−water interfacial adsorption of PFOA, and air−water interfacial areas. The total organic carbon and metal (Fe and Mn) oxide contents of the sand are 0.04% and 227 μg/g, respectively. Solutions were prepared with de-aired and deionized water. All solutions were prepared with 0.01 M NaCl as the background electrolyte.

Surface-Tension Measurements. A De Nouy ring tensiometer (Shanghai HengPing Instrument and Meter Factory, BZY-4B) was used to measure aqueous surface tension based on standard methods. A known mass weight was used to calibrate the tensiometer before experiments. Each sample was measured multiple times until at least three stable measurements were obtained. All surface-tension measurements were conducted at room temperature (~23 °C). Two approaches were used for investigating the impact of SDS on PFOA surface activity, one using a constant ratio of PFOA and SDS (ratios are 10:1, 1:1, and 1:10) and the other using a fixed concentration of SDS (SDS = 1, 10, and 100 μg/L). These measurements are described in detail in the Supporting Information.

Miscible-Displacement Column Experiments. Miscible-displacement experiments were conducted in duplicate with 15 cm long and 2.5 cm inner diameter acrylic columns. All columns were dry packed with sand to obtain uniform consistent bulk densities (mean = 1.56 ± 0.006 g/cm^3) and porosities (mean = 0.476 ± 0.008). Stainless steel sintered wire mesh (#80) was placed on both the bottom and top of the column in contact with the porous media to provide support. The column was oriented vertically during all experiments. High-density polyethylene tubing connected a precision high-performance liquid chromatography (HPLC) pump to the column. Samples were collected in polypropylene tubes using an automated fraction collector. Solutions for all experiments contained 0.01 M NaCl. The measured effluent concentrations were used to develop breakthrough curves, with the measured effluent concentration divided by the input concentration to

https://doi.org/10.1021/acs.est.1c01919
Environ. Sci. Technol. XXXX, XXX, XXX−XXX

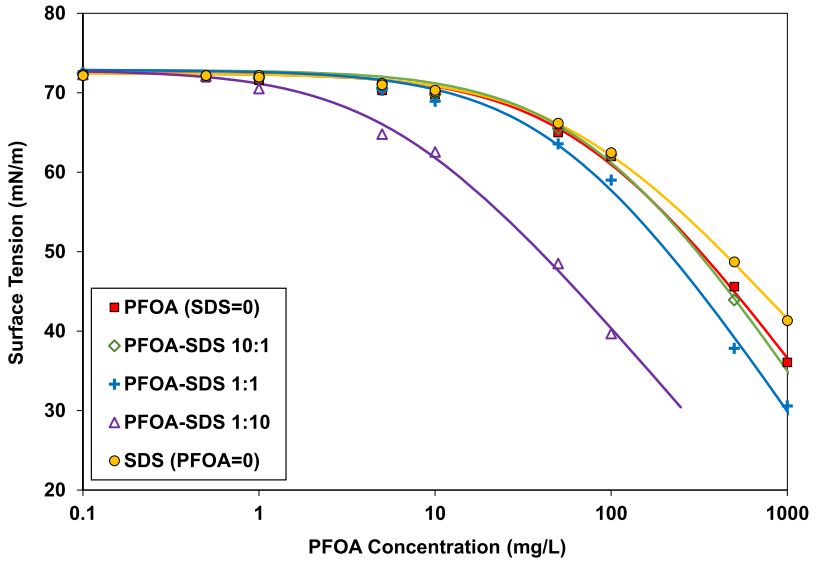

Figure 1. Measured surface tensions for PFOA, SDS, and mixed PFOA–SDS in 0.01 M NaCl solutions. SDS is present in concentrations of constant ratio to PFOA for the mixed-surfactant solutions. Only the concentrations of PFOA are used to plot the mixed-solution data sets. For the SDS (PFOA = 0) data set, the reported concentration is that of SDS. The data points represent the mean of at least three measurements. Error bars for the 95% confidence intervals are smaller than the size of the data-point symbols. The solid curves represent fits obtained with the Szyszkowski equation. Only the ≥0.1 mg/L concentration data are shown to better visualize the differences in surface tensions.

determine the relative concentration. Non-dimensional time was represented as pore volumes, which is defined as the quotient of the column discharge and the water-filled pore-volume capacity of the packed column. Retardation factors were determined for the transport experiments by moment analysis of the breakthrough curves and not by model calibration. Details of the approach and methods are provided in the Supporting Information.

Analytical Methods. The NRT samples were analyzed at a wavelength of 262 nm using ultraviolet–visible spectrophotometry (Unico, model 2008A). PFOA was analyzed directly via liquid chromatography with tandem mass spectrometry (LC–MS/MS) using two methods. First, the PFOA samples without SDS employed Thermo UltiMate 3000 HPLC (Thermo Fisher Scientific, Bremen, Germany) and a AB-Sciex QTRAP 4500 mass spectrometer (AB Sciex Pte. Ltd., Singapore). A Waters column (C18, 2.1 × 50 mm, 1.7 μm) was maintained at 35 °C. The mobile phase of water and 100% acetonitrile applied in the ratio of 40/60 (v/v) was set at a flow rate of 0.25 mL/min. Second, PFOA samples with SDS employed an Agilent HPLC 1260 and a mass spectrometer 6150. An Agilent ZORBAX RRHD Eclipse Plus C18 column (2.1 × 50 mm, 1.8 μm) was maintained at 40 °C. The mobile phase of 0.01 M ammonium acetate and 100% acetonitrile applied in the ratio of 60/40 (v/v) was set at a flow rate of 0.3 mL/min. All the samples were passed through a 0.45 μm filter to remove suspended particulate impurities. Mass-labeled internal standard $^{13}C_4$-PFOA was added to monitor recovery. The R^2 of the calibration curves were >0.999 for each measurement. The quantifiable detection limit of the two systems is ~0.1 μg/L. These methods have been used successfully in our prior studies.[26,33,34]

Mathematical Modeling. A one-dimensional numerical model that couples transient, variably saturated flow, advective and dispersive transport, nonlinear and rate-limited solid-phase and air–water interfacial adsorption, as well as surfactant-induced flow is employed to simulate the PFOA transport experiments.[20] The model is further extended here to account for multiple-component transport of surfactants with competitive adsorption at the air–water interfaces using the multicomponent Langmuir adsorption isotherm[44,45]

$$K_{ia,i} = \frac{\gamma_{0b_i}}{R_g T} \frac{1/a_i}{1 + \sum_{j=1}^{m} C_j/a_j} \quad (1)$$

where a_i and b_i are the Szyskowski parameters determined from the surface-tension data of the individual surfactant component, that is, eq S1 recovers eqs S2 and S3 in Supporting Information for a single-component surfactant when m = 1. The model is used to produce independently predicted simulations of PFOA transport that will be compared to the measured breakthrough curves obtained from the transport experiments. Values for all input parameters are obtained independently, such that no model fitting or calibration is conducted. Details of the mathematical modeling, including the governing equations, input parameters, and operational conditions, are described in the Supporting Information. A simplified transport model is used to simulate the NRT data that accounts for advective–dispersive transport. The model was calibrated to the measured NRT breakthrough curves with one parameter (Peclet number, P) optimized, where $P = vL/D$ (v is the mean porewater velocity, L is the column length, and D is the dispersion coefficient).

RESULTS AND DISCUSSION

Surface-Tension Measurements. The surface tensions measured for PFOA in 0.01 M NaCl solution as a function of aqueous concentration are presented in Figure 1. It is observed that the Szyszkowski equation provides excellent fits to all of the measured data sets (see Table S1 in Supporting Information). The PFOA-alone data are consistent with our prior reported data sets.[26,46] For example, Brusseau[46] presented several surface-tension data sets measured for PFOA in 0.01 M NaCl solution. The Szyszkowski variables for that combined data set (a = 71.4; b = 0.20) are very similar to those determined for the data presented in Figure 1. The

https://doi.org/10.1021/acs.est.1c01919
Environ. Sci. Technol. XXXX, XXX, XXX–XXX

Table 1. Results of Transport Experiments[a]

input concentration (μg/L)								
PFOA	SDS	water saturation	measured R	predicted R[b]	K_d (L/kg)	F_{AWIA}	K_{ia} from breakthrough curve (cm)	K_{ia} from surface tension (cm)[c]
10		1	1.17		0.052			
10	1	1	1.18		0.054			
10	10	1	1.36		0.114			
10	100	1	1.35		0.114			
10		0.65	2.39	2.31		0.81	0.0036	0.0032
10	1	0.67	2.41	2.44		0.71	0.0036	0.0030
10	10	0.67	2.92	2.92		0.67	0.0046	0.0046
10	100	0.68	3.59	9.08		0.79	0.0086	0.0319

[a]Values represent the means of replicate experiments (n = 2). [b]R values predicted for unsaturated-flow PFOA experiments using the K_{ia} values determined from the constant-ratio surface-tension data. [c]Constant PFOA–SDS ratio data.

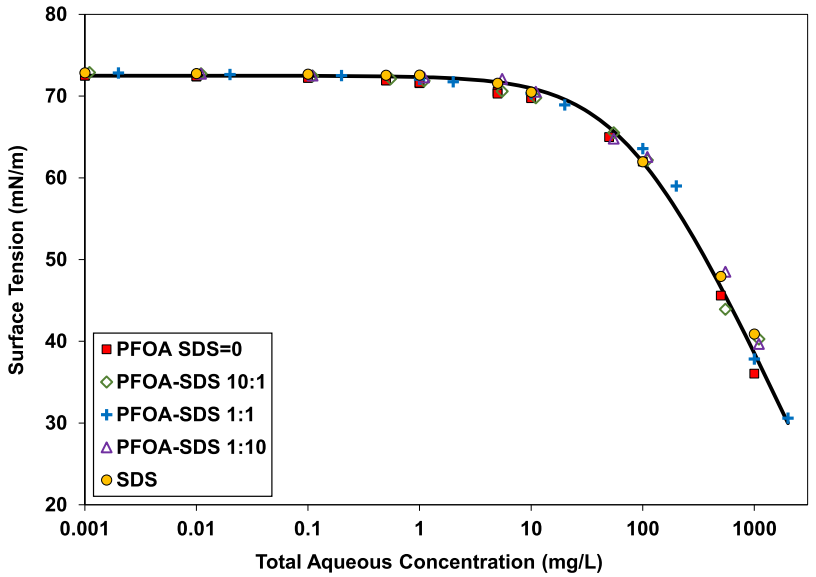

Figure 2. Measured surface tensions for PFOA, SDS, and mixed PFOA–SDS in 0.01 M NaCl solutions. Aqueous concentrations are presented as the combined total of PFOA and SDS for the mixed-surfactant solutions. SDS is present in concentrations of constant ratio to PFOA for the mixed-surfactant solutions. Error bars for the 95% confidence intervals are smaller than the size of the data-point symbols. The solid curve represents the fit obtained with the Szyszkowski equation.

surface tensions for SDS are also presented in Figure 1. Comparison of the two data sets shows that PFOA and SDS have generally similar surface activities. The addition of SDS at a concentration 10-times lower than that of PFOA (PFOA–SDS ratio of 10:1) has minimal impact on the surface tension. The addition of SDS at equal concentration to that of PFOA (1:1 ratio) has a relatively minor impact (Figure 1). Conversely, the addition of SDS at concentrations 10-times higher than that of PFOA (1:10 ratio) significantly increases the surface activity of the solution.

The plots of the constant-ratio surface tensions for the mixed-surfactant solutions presented in Figure 1 are developed using only the PFOA aqueous concentration. However, in this system, the observed change in surface activity results from the combined effect of changes in the concentration of both PFOA and SDS. The mixed-surfactant data can alternatively be plotted employing total surfactant concentration to characterize the change in surface activity as a function of the change in both PFOA and SDS. The data plotted with this standard approach are presented in Figure 2. Inspection of the figure shows that the surface-tension curves for the PFOA–SDS data are essentially coincident with the PFOA-alone and SDS-alone curves. This concurrency demonstrates that surface-activity behavior is consistent among the systems. The surface tensions for PFOA with the fixed concentrations of SDS are essentially identical to that of PFOA with no SDS present (see Figure S1).

Air–water interfacial adsorption coefficients are determined from the measured surface-tension data, as described in the Supporting Information. The values are reported in Table 1 for the constant-ratio data with aqueous concentration set to that of PFOA. A target aqueous concentration of 10 μg/L is employed for the calculations to match the input concentrations used for the transport experiments. A K_{ia} value of 0.0032 cm is determined for PFOA in the absence of SDS. Brusseau[46] compiled 10 individual measured surface-tension data sets for PFOA in 0.01 M NaCl solution and determined a mean K_{ia} from separate analysis of each of the 10 data sets. The mean is 0.0032 cm (0.0024–0.0040, 95% confidence interval) for a selected concentration of 10 μg/L. Notably, the K_{ia} value determined in this study is identical to the mean value determined from the prior study. The K_{ia} value determined for SDS is 0.002 cm, slightly smaller than the value for PFOA.

https://doi.org/10.1021/acs.est.1c01919
Environ. Sci. Technol. XXXX, XXX, XXX–XXX

The K_{ia} value for the 10:1 PFOA−SDS solution is essentially identical to that without SDS, indicating no measurable impact of SDS. The K_{ia} value for the 1:1 PFOA−SDS solution is slightly larger than the prior two values. Conversely, the K_{ia} value for the 1:10 PFOA−SDS solution is significantly larger, consistent with the greatly increased surface activity.

K_{ia} values were also calculated using the constant-ratio surface-tension data with aqueous concentration plotted in terms of the total surfactant (PFOA + SDS). The values are presented in Figure 3 as a function of the PFOA mole fraction.

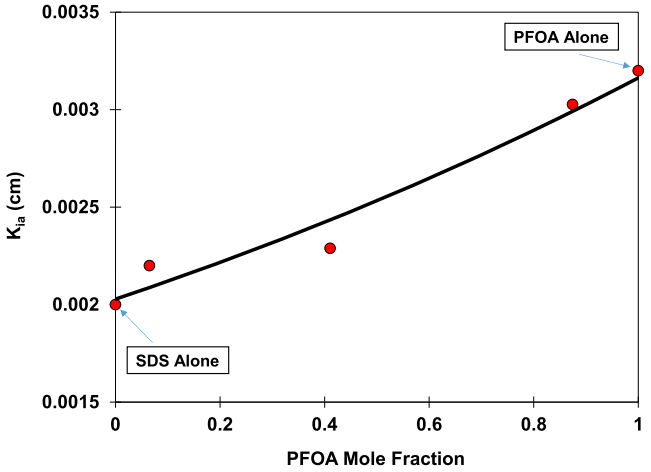

Figure 3. Air−water interfacial adsorption coefficients (K_{ia}) for mixed surfactant (PFOA + SDS) solutions as a function of PFOA mole fraction. The solid curve represents a fit of an exponential function to the measured values, which is used for visualization purposes.

The values for the mixed-surfactant solutions reside within the bounds of the respective K_{ia} values for the PFOA-alone and SDS-alone solutions. The change in K_{ia} is observed to be a function of the mole-fraction composition, consistent with anticipated behavior for a two-component system. A continuous monotonic change in the magnitude of adsorption as a function of the mole fraction, as observed in Figure 3, is considered to be indicative of uniform mixing within the adsorbed layer at the interface (e.g., refs 47 and 48).

NRT Transport. The breakthrough curves for transport of the NRT in the water-saturated packed columns are presented in Figure 4. The data from the different experiments are essentially coincident, indicating excellent reproducibility. The curves are observed to appear in the effluent at one pore volume, signifying no measurable retention. They are symmetrical, with minimal spreading and no evidence of preferential-flow effects. Simulations produced with an ideal 1D advection−dispersion model provide good fits to the data. These results indicate ideal hydrodynamic transport conditions for the packed columns. A dispersivity of 0.12 cm was determined from the modeling.

The breakthrough curves for transport of the NRT in the unsaturated packed columns are also presented in Figure 4. Again, the data from the different experiments are essentially coincident. The curves exhibit measurably greater spreading compared to that of the saturated-column data. This reflects the impact of unsaturated conditions and the presence of fully and partially drained pore sequences on flow and solute transport. The simple transport model still provides a good fit to the measured data but with a larger calibrated dispersivity of 0.42 cm. The results for both saturated and unsaturated conditions are consistent with those reported for transport of the same NRT in the same sand in a prior study.[30]

PFOA Transport under Saturated Conditions. The breakthrough curves for transport of PFOA under saturated-flow conditions exhibit a small magnitude of retardation compared to the NRT, due to sorption by the sand. The breakthrough curves exhibit a small degree of asymmetry and concentration tailing (see Figures 5−7). The transport model incorporating two-domain nonlinear rate-limited sorption provides good simulations of the measured data. Comparisons of simulations including and excluding nonlinear sorption show that there is minimal impact of nonlinear sorption on the asymmetry and tailing, indicating that rate-limited sorption is

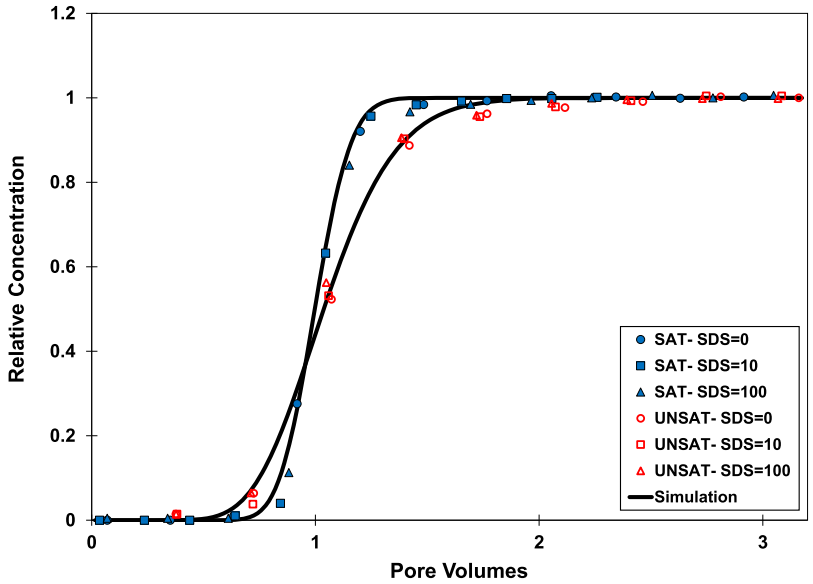

Figure 4. Breakthrough curves for transport of the NRT in the saturated (SAT) and unsaturated (UNSAT) packed columns. The SDS designations listed in the legend refer to the experiment for which each tracer test was conducted. No SDS was present in the NRT solutions. The black curves represent simulations of NRT transport produced with the mathematical model described in the text.

https://doi.org/10.1021/acs.est.1c01919
Environ. Sci. Technol. XXXX, XXX, XXX−XXX

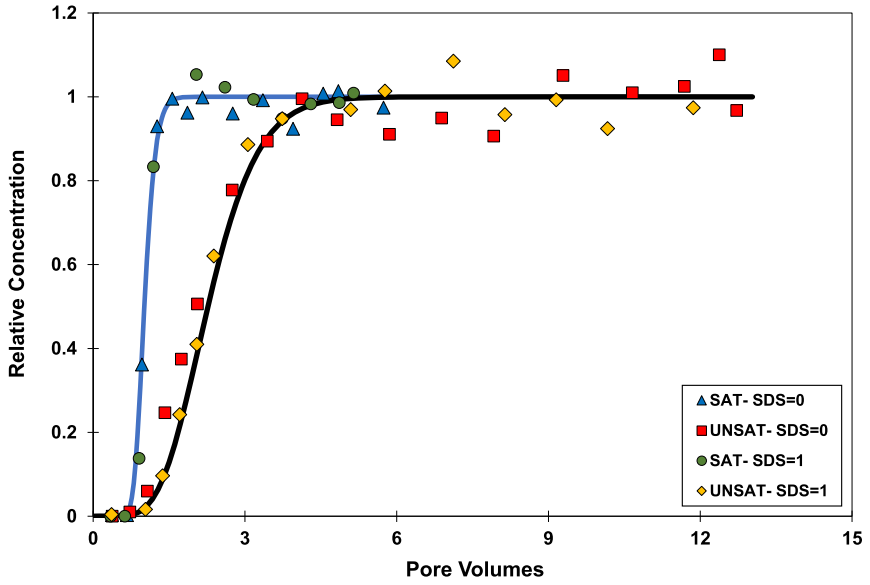

Figure 5. Breakthrough curves for transport of PFOA in sand under saturated (SAT) and unsaturated (UNSAT) conditions. SDS is absent from solution for the first set (SDS = 0) and present in the solution at a fixed concentration of 1 μg/L for the second set (SDS = 1). The curves represent simulations of PFOA transport produced with the mathematical models described in the text. The simulations presented for unsaturated conditions represent an independent prediction with all input parameters obtained independently. Only the arrival fronts are presented to focus on the differences between transport under saturated and unsaturated conditions.

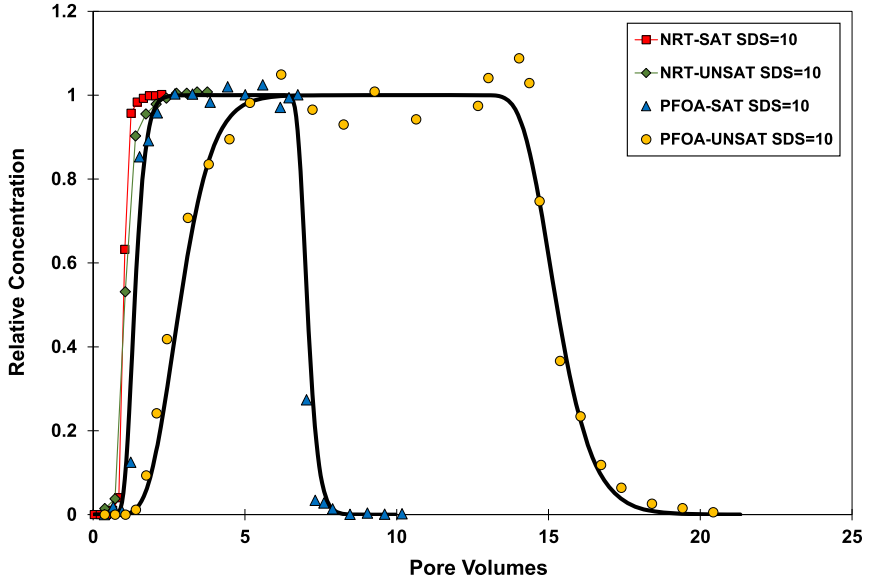

Figure 6. Breakthrough curves for transport of the NRT and PFOA in sand under saturated (SAT) and unsaturated (UNSAT) conditions. SDS is present in the PFOA solution at a fixed concentration of 10 μg/L. The black curves represent simulations of PFOA transport produced with the mathematical models described in the text. The simulation presented for unsaturated conditions represents an independent prediction with all input parameters obtained independently.

the primary cause of the nonideal transport. These results are consistent with prior PFAS transport data.[24,30]

Retardation factors and K_d values determined from moment analysis of the breakthrough curves are reported in Table 1. Notably, the K_d value for PFOA sorption by the sand with no SDS present is consistent with our prior measurements from batch and column isotherm experiments.[29] In addition, the results are consistent with those reported by other investigators who have conducted PFOA transport experiments with PFOA and the same sand, as discussed in Wang et al.[31]

The K_d value for PFOA sorption by the sand with SDS = 1 μg/L is the same as that with no SDS present. This indicates that the presence of very low levels of SDS has no impact on PFOA sorption. Conversely, the K_d values for PFOA sorption with SDS present at 10 and 100 μg/L are approximately twice as large compared to no SDS present, which suggests that there may be a relatively small degree of enhanced sorption.

PFOA Transport under Unsaturated Conditions. Breakthrough curves for transport of PFOA under unsaturated conditions exhibit significantly greater magnitudes of retardation compared to PFOA transport under saturated conditions (Figures 5−7). The additional retention is associated with adsorption at the air−water interface. Greater retardation is observed for PFOA with increasing concentrations of SDS

https://doi.org/10.1021/acs.est.1c01919
Environ. Sci. Technol. XXXX, XXX, XXX−XXX

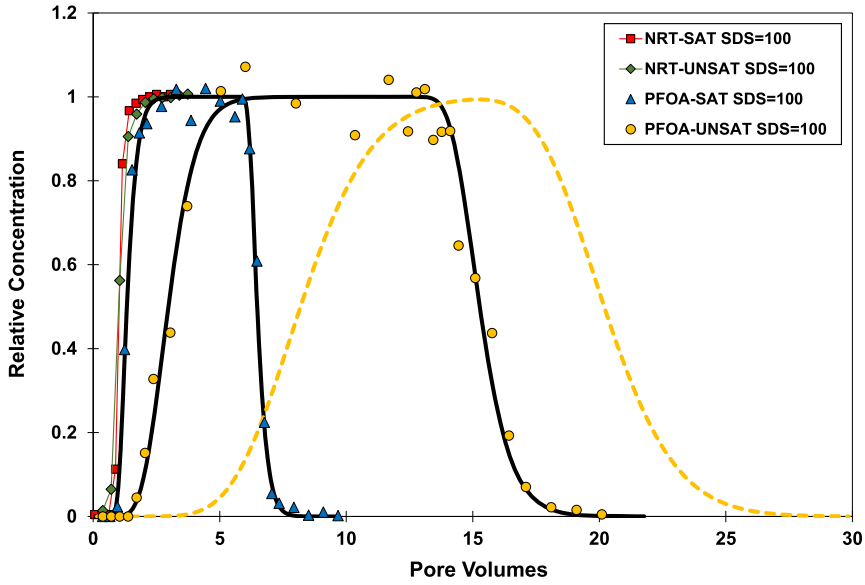

Figure 7. Breakthrough curves for transport of the NRT and PFOA in sand under saturated (SAT) and unsaturated (UNSAT) conditions. SDS is present in the PFOA solution at a fixed concentration of 100 μg/L. The black curves represent simulations of PFOA transport produced with the mathematical models described in the text. Three different approaches are used to determine air−water interfacial adsorption of PFOA for the unsaturated-flow experiment. (1) Dashed yellow curve represents the independently predicted simulation produced with K_{ia} determined from the constant-ratio surface-tension data. (2) Independently predicted curve produced using the multiple-component Langmuir adsorption model is identical to the yellow-dashed curve. (3) Solid black curve is produced by scaling the K_{ia} determined from the surface-tension data.

present (see TOC graphic). The retardation factor for PFOA with SDS = 1 μg/L (R = 2.4) is essentially identical to that for PFOA with no SDS (Table 1). Additionally, the two breakthrough curves are essentially coincident (Figure 5). Conversely, the retardation factor for PFOA with SDS = 10 μg/L is 2.9, measurably larger than that for the experiment with no SDS. Furthermore, the retardation factor for the SDS = 100 μg/L experiment is 3.6, still larger than those measured for the other experiments. The values for the fraction of measured retention associated with air−water interfacial adsorption (F_{AWIA}, defined by eq S6 in Supporting Information) for the four systems range from 0.67 to 0.81, signifying that air−water interfacial adsorption contributes the majority of PFOA retention for all cases (Table S2).

The increased retardation observed for PFOA under unsaturated-flow conditions in the presence of SDS indicates that the transport of PFOA experiences enhanced retention in the presence of higher levels of SDS. As discussed in the preceding subsection, the presence of 10 and 100 μg/L SDS caused enhanced sorption of PFOA. However, the sorption was increased by a factor of 2, which would contribute to only a relatively minor increase in retardation under unsaturated conditions given that air−water interfacial adsorption contributes the majority of retention for PFOA transport. Discussion of the surface-tension data and associated K_{ia} values revealed greater air−water interfacial adsorption of PFOA in the presence of higher ratios of SDS. This enhancement provides the primary source of the increased retardation observed for PFOA transport under unsaturated conditions.

The impact of enhanced air−water interfacial adsorption can be examined in more detail by comparing the K_{ia} values determined from the transport experiments. Air−water interfacial adsorption coefficients determined from analysis of the PFOA breakthrough-curve data, as described in Supporting Information, are reported in Table 1. The K_{ia} value determined from the transport experiments for PFOA with no SDS present is 0.0036 cm. This value is statistically identical to transport-based K_{ia} values measured for PFOA in our prior studies for the same concentration of 10 μg/L.[26,33,46] Specifically, Brusseau[46] reported a mean transport-measured value of 0.0033 (0.0028−0.0038) cm, with the 95% confidence interval determined from seven measurements. This consistency illustrates excellent reproducibility of the experiment methods and analyses.

The K_{ia} value determined from the transport experiments for PFOA with SDS = 1 μg/L is 0.0036 cm. This indicates that there is no impact of SDS on air−water interfacial adsorption during PFOA transport, which is consistent with the surface-tension measurements. The K_{ia} values for the SDS = 10 and 100 μg/L experiments are 0.0046 and 0.0086 cm, respectively. These two values are outside of the 95% confidence interval reported above for PFOA alone. Notably, the two values are larger than the PFOA-alone value, indicating enhanced adsorption of PFOA at the air−water interface in the presence of SDS. Again, this is consistent with the greater surface activities observed from the constant-ratio surface-tension measurements.

The K_{ia} value determined from the transport experiment for PFOA with no SDS present is very similar to the value determined from the corresponding surface-tension data (Table 1). This is also the case for the K_{ia} values measured for the SDS = 1 and 10 μg/L experiments. The consistency of K_{ia} values measured from transport experiments and surface-tension data has been demonstrated in our prior studies,[24,30,46] as illustrated by the two sets of coincident means and 95% confidence intervals referred to in the preceding discussion. As a result of the consistency of the two sets of K_{ia} values, the predicted retardation factors obtained for PFOA using the constant-ratio surface-tension data are very similar (within measurement uncertainty) to the measured values (see Table 1). Conversely, the K_{ia} value for the SDS = 100 μg/L transport experiment is smaller than the value determined from the

https://doi.org/10.1021/acs.est.1c01919
Environ. Sci. Technol. XXXX, XXX, XXX−XXX

surface-tension data, and the predicted retardation factor is much larger than the measured value. This will be discussed in the following section.

Mathematical Modeling of Transport under Unsaturated Conditions. The simulations produced with the mathematical model for PFOA transport under unsaturated conditions with and without SDS provide very good representations of the measured breakthrough curves. This is illustrated in Figure 5 for the case with no SDS present and with SDS present at 1 μg/L and Figures 6 and 7 for the cases with SDS present at 10 and 100 μg/L, respectively. The mean R^2 value for the simulations is 0.96, and the root-mean-square-error values were all <0.1. Notably, surfactant-induced flow was demonstrated to be insignificant for all cases, which was anticipated based on the experiment conditions (low solute concentrations). This is consistent with our prior simulations of miscible-displacement transport data for PFAS.[49]

Simulations conducted with air−water interfacial adsorption treated as nonlinear versus linear were essentially identical. This reflects the fact that the K_{ia} values exhibited minimal change during transport for all nonlinear simulations cases, reflecting that the input concentrations used for the experiments are below the critical concentration wherein K_{ia} attains an essentially constant maximum value.[46,50] As a result, air−water interfacial adsorption is approximately linear for the conditions of the experiments. This is illustrated by the observed shapes of the measured and simulated breakthrough curves. The curves are relatively symmetrical and do not exhibit any pronounced self-sharpening of the arrival front or enhanced spreading of the elution front (see Figures 6 and 7). This is also consistent with prior simulations of PFAS transport data.[30,35,49]

The simulations presented in Figures 5 and 6 for PFOA transport under unsaturated conditions, in the absence of SDS and in the presence of 1 or 10 μg/L SDS, represent predictions wherein values for all input parameters were obtained independently. The good match between independently predicted simulations and measured data indicates that the model provides a robust representation of the relevant processes influencing transport. It also indicates that the input values are accurate. This includes the use of the measured surface-tension functions to represent air−water interfacial adsorption. Hence, these results demonstrate that surface-tension measurements provided an accurate, robust representation of surface activity and interfacial adsorption for transport conditions for these three cases. This is consistent with the discussion above regarding similarity of transport and surface-tension-determined K_{ia} values and with our prior studies of single-solute PFAS transport.[30,34,35] Recent discussion has focused on the magnitude of air−water interfacial adsorption of PFAS at lower concentrations, with speculation that K_{ia} values determined from surface-tension data may not be representative under lower-concentration conditions.[51,52] The results of the present study and those of prior recent studies show that K_{ia} values determined from surface-tension data are representative of air−water interfacial adsorption for PFAS transport in unsaturated porous media.[26,30,34,35,46]

In contrast to the first three cases, the transport of PFOA in the presence of 100 μg/L of SDS could not be predicted using the measured surface-tension data. This is shown in Figure 7, wherein use of the K_{ia} determined from the constant-ratio surface-tension data results in significantly greater simulated retention compared to that of the measured. This indicates a disparity in the characterization of interfacial adsorption between the batch surface-tension system and the transport system. Investigating the possible reasons for this disparity requires an examination of the relative magnitudes of retention of PFOA and SDS and the resultant potential for differential transport, that is, chromatographic separation, of the co-solutes. For example, if two co-solutes have similar magnitudes of retention, they are anticipated to exhibit relatively concurrent transport. Conversely, differential rates of transport and chromatographic separation are expected if they have significantly different magnitudes of retention. This process was discussed, for example, with regard to transport experiments conducted for SDS and sodium dodecylbenzenesulfonate transport in quartz sand and sandy soil.[38] The occurrence of differential transport means that the concentrations of both solutes will differentially change over time and also that the spatial distributions within the porous medium with respect to each other will also be variable. In other words, the concentration ratios of PFOA and SDS are likely to change with time and location. This dynamic condition would be difficult to represent by standard surface-tension measurements, either using constant ratios or fixed concentrations of SDS.

The results of the simulations show that PFOA and SDS experienced differential transport during the experiments. The degree of differential transport varied among the three systems, corresponding to the relative magnitudes of retardation (see Figure S2 in Supporting Information). This can be readily discussed in terms of retardation factors. The respective retardation factors for PFOA and SDS are 2.4−6.2, 2.9−5.2, and 3.3−4.1 for the SDS = 1, 10, and 100 μg/L experiments, respectively. Hence, some portion of the leading edge of the PFOA pulse would have separated from the SDS pulse during transport. This separation was greatest for the SDS = 1 μg/L experiment (<50%) and least for the 100 μg/L experiment (<15%). With these results in mind, the different approaches for representing air−water interfacial adsorption were investigated by conducting a series of simulations employing different inputs for the K_{ia} function for the SDS = 100 μg/L data.

One approach is to use the multiple-component Langmuir adsorption model (eq 1). This approach employs the single-solute surface-tension data measured for PFOA and SDS. The simulations including multiple-component adsorption were essentially identical to those produced with the single-component model for all three PFOA−SDS systems (see Figure 7 for an example). This indicates that there was no appreciable impact of standard competitive effects on air−water interfacial adsorption for any of the three PFOA−SDS systems. This is consistent with the results of the surface tensions measured for PFOA with fixed SDS concentrations. Competitive adsorption is not expected for the low SDS concentrations employed in the experiments based on the standard multiple-component Langmuir model. While this approach was accurate in terms of predicting no competitive effects, none of which were observed for the measured data, it clearly fails to predict the enhanced air−water interfacial adsorption observed for PFOA transport in the presence of higher SDS concentrations (see Figure 7).

The results presented above demonstrate that the presence of SDS at the highest concentration had an impact on air−water interfacial adsorption of PFOA under transport conditions that could not be predicted based on surface-

https://doi.org/10.1021/acs.est.1c01919
Environ. Sci. Technol. XXXX, XXX, XXX−XXX

tension characterization. For this system, the surface-tension function needed to be scaled to produce an effective K_{ia} to represent the observed enhanced air−water interfacial adsorption. The multiple-component Langmuir adsorption model is based on an assumption of no interactions among the PFOS and SDS monomers in solution or at the interface. Thus, it does not capture potential synergistic multiple-component interactions that may impact air−water interfacial adsorption in a transport system.

Implications. The results of this study provide new insights into PFAS transport behavior that may be relevant for sites wherein PFAS and hydrocarbon surfactants co-occur. As demonstrated herein, the presence of hydrocarbon surfactants can lead to enhanced PFAS retention, which would reduce leaching rates in the vadose zone. This in turn would impact the timescale for PFAS retention in the vadose zone and the magnitude of mass discharge to groundwater. The impact of SDS on PFOA adsorption at the air−water interface during transport could not be predicted based on surface-tension data for the highest SDS concentration. The results of this study suggest that it is critical to characterize the concentration profiles of both PFAS and hydrocarbon surfactants at AFFF and other sites to improve characterization and modeling of PFAS migration. Additional research is warranted to investigate the potential impacts of other hydrocarbon surfactants on PFOA and other PFAS for a variety of porous media.

■ ASSOCIATED CONTENT

Supporting Information

The Supporting Information is available free of charge at https://pubs.acs.org/doi/10.1021/acs.est.1c01919.

Selection of SDS as the co-solute, selection of PFOA concentration, surface-tension measurements, miscible-displacement column experiments, LC−MS/MS methods, data analysis, mathematical modeling, Szyszkowski equation parameters for surface-tension measurements, column experiments for PFOA and NRTs, measured surface tensions for PFOA with fixed SDS, and predicted breakthrough curves for PFOA and SDS transport under unsaturated conditions (PDF)

■ AUTHOR INFORMATION

Corresponding Authors

Ni Yan − *Key Laboratory of Marine Environmental Science and Ecology, Ministry of Education, College of Environmental Science and Engineering, Ocean University of China, Qingdao 266100, P. R. China; College of Environmental Science and Engineering, Ocean University of China, Qingdao 266100, China;* orcid.org/0000-0002-7390-3804; Email: yanni@ouc.edu.cn

Mark L. Brusseau − *Environmental Science Department and Department of Hydrology and Atmospheric Sciences, University of Arizona, Tucson, Arizona 85721, United States;* orcid.org/0000-0002-6937-2975; Email: Brusseau@arizona.edu

Authors

Yifan Ji − *Key Laboratory of Marine Environmental Science and Ecology, Ministry of Education, College of Environmental Science and Engineering, Ocean University of China, Qingdao 266100, P. R. China; College of Environmental Science and Engineering, Ocean University of China, Qingdao 266100, China*

Bo Guo − *Department of Hydrology and Atmospheric Sciences, University of Arizona, Tucson, Arizona 85721, United States;* orcid.org/0000-0002-8825-7331

Xilai Zheng − *Key Laboratory of Marine Environmental Science and Ecology, Ministry of Education, College of Environmental Science and Engineering, Ocean University of China, Qingdao 266100, P. R. China; College of Environmental Science and Engineering, Ocean University of China, Qingdao 266100, China*

Mengfan Dai − *Key Laboratory of Marine Environmental Science and Ecology, Ministry of Education, College of Environmental Science and Engineering, Ocean University of China, Qingdao 266100, P. R. China; College of Environmental Science and Engineering, Ocean University of China, Qingdao 266100, China*

Hejie Liu − *Key Laboratory of Marine Environmental Science and Ecology, Ministry of Education, College of Environmental Science and Engineering, Ocean University of China, Qingdao 266100, P. R. China; College of Environmental Science and Engineering, Ocean University of China, Qingdao 266100, China*

Xin Li − *Key Laboratory of Marine Environmental Science and Ecology, Ministry of Education, College of Environmental Science and Engineering, Ocean University of China, Qingdao 266100, P. R. China; College of Environmental Science and Engineering, Ocean University of China, Qingdao 266100, China*

Complete contact information is available at: https://pubs.acs.org/10.1021/acs.est.1c01919

Notes

The authors declare no competing financial interest.

■ ACKNOWLEDGMENTS

This research was funded by the National Natural Science Foundation of China (no. 41907161), the China Postdoctoral Science Foundation (no. 2019M662448), and the Shandong Postdoctoral Innovation Project (no. 202001013), with additional support provided by the NIEHS Superfund Research Program (grant #P42 E504940) and the National Science Foundation (2023351). We thank the reviewers for their constructive comments.

■ REFERENCES

(1) Li, F.; Duan, J.; Tian, S.; Ji, H.; Zhu, Y.; Wei, Z.; Zhao, D. Short-chain per- and polyfluoroalkyl substances in aquatic systems: Occurrence, impacts and treatment. *Chem. Eng. J.* **2020**, *380*, 122506.

(2) Cai, M.; Zhao, Z.; Yin, Z.; Ahrens, L.; Huang, P.; Cai, M.; Yang, H.; He, J.; Sturm, R.; Ebinghaus, R.; Xie, Z. Occurrence of perfluoroalkyl compounds in surface waters from the North Pacific to the Arctic Ocean. *Environ. Sci. Technol.* **2012**, *46*, 661−668.

(3) Prevedouros, K.; Cousins, I. T.; Buck, R. C.; Korzeniowski, S. H. Sources, Fate and Transport of Perfluorocarboxylates. *Environ. Sci. Technol.* **2006**, *40*, 32−44.

(4) Rankin, K.; Mabury, S. A.; Jenkins, T. M.; Washington, J. W. A North American and global survey of perfluoroalkyl substances in surface soils: Distribution patterns and mode of occurrence. *Chemosphere* **2016**, *161*, 333−341.

(5) Brusseau, M. L.; Anderson, R. H.; Guo, B. PFAS concentrations in soils: Background levels versus contaminated sites. *Sci. Total Environ.* **2020**, *740*, 140017.

(6) Weber, A. K.; Barber, L. B.; LeBlanc, D. R.; Sunderland, E. M.; Vecitis, C. D. Geochemical and Hydrologic Factors Controlling Subsurface Transport of Poly- and Perfluoroalkyl Substances, Cape Cod, Massachusetts. *Environ. Sci. Technol.* **2017**, *51*, 4269−4279.
(7) McGuire, M. E.; Schaefer, C.; Richards, T.; Backe, W. J.; Field, J. A.; Houtz, E.; Sedlak, D. L.; Guelfo, J. L.; Wunsch, A.; Higgins, C. P. Evidence of remediation-induced alteration of subsurface poly- and perfluoroalkyl substance distribution at a former firefighter training area. *Environ. Sci. Technol.* **2014**, *48*, 6644−6652.
(8) Moody, C. A.; Hebert, G. N.; Strauss, S. H.; Field, J. A. Occurrence and persistence of perfluorooctanesulfonate and other perfluorinated surfactants in groundwater at a fire-training area at Wurtsmith Air Force Base, Michigan, USA. *J. Environ. Monit.* **2003**, *5*, 341−345.
(9) Adamson, D. T.; Nickerson, A.; Kulkarni, P. R.; Higgins, C. P.; Popovic, J.; Field, J.; Rodowa, A.; Newell, C.; DeBlanc, P.; Kornuc, J. J. Mass-Based, Field-Scale Demonstration of PFAS Retention within AFFF-Associated Source Areas. *Environ. Sci. Technol.* **2020**, *54*, 15768−15777.
(10) Anderson, R. H.; Adamson, D. T.; Stroo, H. F. Partitioning of poly- and perfluoroalkyl substances from soil to groundwater within aqueous film-forming foam source zones. *J. Contam. Hydrol.* **2019**, *220*, 59−65.
(11) Moody, C. A.; Field, J. A. Perfluorinated Surfactants and the Environmental Implications of Their Use in Fire-Fighting Foams. *Environ. Sci. Technol.* **2000**, *34*, 3864−3870.
(12) Vecitis, C. D.; Wang, Y.; Cheng, J.; Park, H.; Mader, B. T.; Hoffmann, M. R. Sonochemical Degradation of Perfluorooctanesulfonate in Aqueous Film-Forming Foams. *Environ. Sci. Technol.* **2010**, *44*, 432−438.
(13) Hill, C.; Czajka, A.; Hazell, G.; Grillo, I.; Rogers, S. E.; Skoda, M. W. A.; Joslin, N.; Payne, J.; Eastoe, J. Surface and bulk properties of surfactants used in fire-fighting. *J. Colloid Interface Sci.* **2018**, *530*, 686−694.
(14) Houtz, E. F.; Higgins, C. P.; Field, J. A.; Sedlak, D. L. Persistence of perfluoroalkyl acid precursors in AFFF-impacted groundwater and soil. *Environ. Sci. Technol.* **2013**, *47*, 8187−8195.
(15) Barzen-Hanson, K. A.; Roberts, S. C.; Choyke, S.; Oetjen, K.; McAlees, A.; Riddell, N.; McCrindle, R.; Ferguson, P. L.; Higgins, C. P.; Field, J. A. Discovery of 40 Classes of Per- and Polyfluoroalkyl Substances in Historical Aqueous Film-Forming Foams (AFFFs) and AFFF-Impacted Groundwater. *Environ. Sci. Technol.* **2017**, *51*, 2047−2057.
(16) Nickerson, A.; Rodowa, A. E.; Adamson, D. T.; Field, J. A.; Kulkarni, P. R.; Kornuc, J. J.; Higgins, C. P. Spatial Trends of Anionic, Zwitterionic, and Cationic PFASs at an AFFF-Impacted Site. *Environ. Sci. Technol.* **2021**, *55*, 313−323.
(17) García, R. A.; Chiaia-Hernández, A. C.; Lara-Martin, P. A.; Loos, M.; Hollender, J.; Oetjen, K.; Higgins, C. P.; Field, J. A. Suspect Screening of Hydrocarbon Surfactants in AFFFs and AFFFContaminated Groundwater by High-Resolution Mass Spectrometry. *Environ. Sci. Technol.* **2019**, *53*, 8068−8077.
(18) Shin, H.-M.; Vieira, V. M.; Ryan, P. B.; Detwiler, R.; Sanders, B.; Steenland, K.; Bartell, S. M. Environmental fate and transport modeling for perfluorooctanoic acid emitted from the Washington Works Facility in West Virginia. *Environ. Sci. Technol.* **2011**, *45*, 1435−1442.
(19) Xiao, F.; Simcik, M. F.; Halbach, T. R.; Gulliver, J. S. Perfluorooctane sulfonate (PFOS) and perfluorooctanoate (PFOA) in soils and groundwater of a U.S. metropolitan area: Migration and implications for human exposure. *Water Res.* **2015**, *72*, 64−74.
(20) Guo, B.; Zeng, J.; Brusseau, M. L. A Mathematical Model for the Release, Transport, and Retention of Per- and Polyfluoroalkyl Substances (PFAS) in the Vadose Zone. *Water Resour. Res.* **2020**, *56*, No. e2019WR026667.
(21) Brusseau, M. L. Assessing the potential contributions of additional retention processes to PFAS retardation in the subsurface. *Sci. Total Environ.* **2018**, *613−614*, 176−185.
(22) Aly, Y. H.; Liu, C.; McInnis, D. P.; Lyon, B. A.; Hatton, J.; McCarty, M.; Arnold, W. A.; Pennell, K. D.; Simcik, M. F. In Situ Remediation Method for Enhanced Sorption of Perfluoro-Alkyl Substances onto Ottawa Sand. *J. Environ. Eng.* **2018**, *144*, 04018086.
(23) Aly, Y. H.; McInnis, D. P.; Lombardo, S. M.; Arnold, W. A.; Pennell, K. D.; Hatton, J.; Simcik, M. F. Enhanced Adsorption of Perfluoro Alkyl Substances for In situ Remediation. *Environ. Sci. Water Res. Technol.* **2019**, *5*, 1867−1875.
(24) Brusseau, M. L.; Khan, N.; Wang, Y.; Yan, N.; Van Glubt, S.; Carroll, K. C. Nonideal Transport and Extended Elution Tailing of PFOS in Soil. *Environ. Sci. Technol.* **2019**, *53*, 10654−10664.
(25) Guelfo, J. L.; Wunsch, A.; McCray, J.; Stults, J. F.; Higgins, C. P. Subsurface transport potential of perfluoroalkyl acids (PFAAs): Column experiments and modeling. *J. Contam. Hydrol.* **2020**, *233*, 103661.
(26) Lyu, Y.; Brusseau, M. L.; Chen, W.; Yan, N.; Fu, X.; Lin, X. Adsorption of PFOA at the Air-Water Interface during Transport in Unsaturated Porous Media. *Environ. Sci. Technol.* **2018**, *52*, 7745−7753.
(27) Lyu, X.; Liu, X.; Sun, Y.; Ji, R.; Gao, B.; Wu, J. Transport and retention of perfluorooctanoic acid (PFOA) in natural soils: Importance of soil organic matter and mineral contents, and solution ionic strength. *J. Contam. Hydrol.* **2019**, *225*, 103477.
(28) McKenzie, E. R.; Siegrist, R. L.; McCray, J. E.; Higgins, C. P. Effects of chemical oxidants on perfluoroalkyl acid transport in one-dimensional porous media columns. *Environ. Sci. Technol.* **2015**, *49*, 1681−1689.
(29) Van Glubt, S.; Brusseau, M. L.; Yan, N.; Huang, D.; Khan, N.; Carroll, K. C. Column versus batch methods for measuring PFOS and PFOA sorption to geomedia. *Environ. Pollut.* **2021**, *268*, 115917.
(30) Brusseau, M. L.; Yan, N.; Van Glubt, S.; Wang, Y.; Chen, W.; Lyu, Y.; Dungan, B.; Carroll, K. C.; Holguin, F. O. Comprehensive retention model for PFAS transport in subsurface systems. *Water Res.* **2019**, *148*, 41−50.
(31) Wang, Y.; Khan, N.; Huang, D.; Carroll, K. C.; Brusseau, M. L. Transport of PFOS in aquifer sediment: Transport behavior and a distributed-sorption model. *Sci. Total Environ.* **2021**, *779*, 146444.
(32) Lyu, X.; Liu, X.; Sun, Y.; Gao, B.; Ji, R.; Wu, J.; Xue, Y. Importance of surface roughness on per fluorooctanoic acid (PFOA) transport in unsaturated porous media. *Environ. Pollut.* **2020**, *266*, 115343.
(33) Lyu, Y.; Brusseau, M. L. The influence of solution chemistry on air-water interfacial adsorption and transport of PFOA in unsaturated porous media. *Sci. Total Environ.* **2020**, *713*, 136744.
(34) Yan, N.; Ji, Y.; Zhang, B.; Zheng, X.; Brusseau, M. L. Transport of GenX in Saturated and Unsaturated Porous Media. *Environ. Sci. Technol.* **2020**, *54*, 11876−11885.
(35) Brusseau, M. L. Simulating PFAS transport influenced by rate-limited multi-process retention. *Water Res.* **2020**, *168*, 115179.
(36) Brusseau, M. L. Estimating the relative magnitudes of adsorption to solid-water and air/oil-water interfaces for per- and poly-fluoroalkyl substances. *Environ. Pollut.* **2019**, *254*, 113102.
(37) Brusseau, M. L.; Peng, S.; Schnaar, G.; Murao, A. Measuring air−water interfacial areas with X-ray microtomography and interfacial partitioning tracer tests. *Environ. Sci. Technol.* **2007**, *41*, 1956−1961.
(38) Brusseau, M. L.; El Ouni, A.; Araujo, J. B.; Zhong, H. Novel methods for measuring air-water interfacial area in unsaturated porous media. *Chemosphere* **2015**, *127*, 208−213.
(39) Karagunduz, A.; Young, M. H.; Pennell, K. D. Influence of surfactants on unsaturated water flow and solute transport. *Water Resour. Res.* **2015**, *51*, 1977−1988.
(40) Kim, H.; Rao, P. S. C.; Annable, M. D. Determination of effective air-water interfacial area in partially saturated porous media using surfactant adsorption. *Water Resour. Res.* **1997**, *33*, 2705−2711.
(41) Pan, G.; Jia, C.; Zhao, D.; You, C.; Chen, H.; Jiang, G. Effect of cationic and anionic surfactants on the sorption and desorption of perfluorooctane sulfonate (PFOS) on natural sediments. *Environ. Pollut.* **2009**, *157*, 325−330.

https://doi.org/10.1021/acs.est.1c01919
Environ. Sci. Technol. XXXX, XXX, XXX−XXX

(42) Guelfo, J. L.; Higgins, C. P. Subsurface Transport Potential of Perfluoroalkyl Acids at Aqueous Film-Forming Foam (AFFF)-Impacted Sites. *Environ. Sci. Technol.* **2013**, *47*, 4164−4171.
(43) Brusseau, M. L.; Van Glubt, S. The influence of surfactant and solution composition on PFAS adsorption at fluid-fluid interfaces. *Water Res.* **2019**, *161*, 17−26.
(44) Rosen, M. J.; Kunjappu, J. T. *Surfactants and Interfacial Phenomena*; John Wiley & Sons, 2012.
(45) Vecitis, C. D.; Park, H.; Cheng, J.; Mader, B. T.; Hoffmann, M. R. Enhancement of Perfluorooctanoate and Perfluorooctanesulfonate Activity at Acoustic Cavitation Bubble Interfaces. *J. Phys. Chem. C* **2008**, *112*, 16850−16857.
(46) Brusseau, M. L. Examining the robustness and concentration dependency of PFAS air-water and NAPL-water interfacial adsorption coefficients. *Water Res.* **2021**, *190*, 116778.
(47) Matsuki, H.; Ikeda, N.; Aratono, M.; Kaneshina, S.; Motomura, K. Study on the miscibility of lithium tetradecyl sulfate and lithium perfluorooctane sulfonate in the adsorbed film and micelle. *J. Colloid Interface Sci.* **1992**, *154*, 454−460.
(48) Aratono, M.; Ikeguchi, M.; Takiue, T.; Ikeda, N.; Motomura, K. Thermodynamic Study on the Miscibility of Sodium Perfluorooctanoate and Sodium Decyl Sulfate in the Adsorbed Film and Micelle. *J. Colloid Interface Sci.* **1995**, *174*, 156−161.
(49) Brusseau, M. L.; Lyu, Y.; Yan, N.; Guo, B. Low-concentration tracer tests to measure air−water interfacial area in porous media. *Chemosphere* **2020**, *250*, 126305.
(50) Brusseau, M. L. The influence of molecular structure on the adsorption of PFAS to fluid-fluid interfaces: using QSPR to predict interfacial adsorption coefficients. *Water Res.* **2019**, *152*, 148−158.
(51) Arshadi, M.; Costanza, J.; Abriola, L. M.; Pennell, K. D. Comment on "Uptake of Poly- and Perfluoroalkyl Substances at the Air-Water Interface". *Environ. Sci. Technol.* **2020**, *54*, 7019−7020.
(52) Schaefer, C. E.; Nguyen, D.; Field, J. Response to the Comment on "Uptake of Poly- and Perfluoroalkyl Substances at the Air-Water Interface". *Environ. Sci. Technol.* **2020**, *54*, 7021−7022.

https://doi.org/10.1021/acs.est.1c01919
Environ. Sci. Technol. XXXX, XXX, XXX−XXX